River Flow 2010 - Dittrich, Koll, Aberle & Geisenhainer (eds) - © 2010 Bundesanstalt für Wasserbau ISBN 978-3-939230-00-7

Turbulent Flow in a Meander Bend of a Lowland River: field measurements and preliminary results

A. Sukhodolov
Department of Ecohydraulics, Leibnitz Institute of Freshwater Ecology and Inland Fisheries, Berlin, Germany

E. Kaschtschejewa
Geography Department, Humboldt University of Berlin, Germany

ABSTRACT: Many river restoration projects include the reconstruction of meander bends on previously canalized rivers as a primary measure for recovering degraded fluvial ecosystems. Secondary currents evolving on account of channel curvature are the dominant features that alter initially uniform open-channel flow, shape riverbed morphology, and create diverse habitats. Although the flow structure in meander bends was the focus of numerous experimental, theoretical, and numerical research, accurate prediction of flow and up-scaling of experimental results is restricted by the insufficient information about flow in natural rivers. In this paper we report on the field studies that were completed on a meander bend of the lowland river Spree in Germany. Analysis of historical maps revealed that the planar configuration of the meander bend in this study was stable over the period of more then two hundred years. The length of the bend in a centreline is 760 m and the wave length is 485 m. The channel is 30 to 40 m wide with the bathymetry characteristic of meander patterns which includes a riffle-pool sequence. The maximal depth varies from 1.6 m in the riffle to 3.2 m in the pool. Accurate and detailed measurements of three-dimensional velocity vectors were completed in 7 cross-sections uniformly distributed along the meander path. In each cross-section from 12 to 20 verticals each composed of 11 measuring points were measured with the use of acoustic Doppler velocimeters. Preliminary results indicate that the measurements were capable to assess the development of secondary circulations and to investigate their interactions with the shear stresses imposed by friction over the riverbed. The results of this study have direct relation to the studies of benthic invertebrates on the reach (Blettler et al. 2010).

Keywords: Meanders, Secondary flow, Hydrodynamics, Turbulence, Shear layers

1 INTRODUCTION

Meandering pattern is the most widely known feature of a fluvial network which for general public is inevitably associated with a pristine state of rivers. Not surprisingly that river revitalization projects that boomed over the last decade consider re-meandering of canalized and trained river reaches as the primary measure for improving ecosystem services of rivers by enhancing diversity of in-stream habitats (Figure 1). Morphology of meandering channels is extremely heterogeneous and comprised of riffle-pool sequences with zones of shallow and deep water. A complex flow composed of spatially non-uniform primary flow, spiraling secondary flow and areas of separated flow evolves in river bends and facilitates heterogeneity in riverbed substrate distribution and delivery and accumulation of organic carbon.

Although systematic studies of river meandering have been carried out for more than a hundred years and yielded the information relevant for solving many engineering problems (Fargue 1868, Rozovskii 1957, Seminara 2006), further integration of the knowledge on physical processes into the practice of stream ecology necessitates a deeper understanding of turbulent flow structure in natural streams and its relation to the biotic component of ecosystems. Recently Leibniz Institute of Freshwater Ecology and Inland Fisheries (IGB, Germany), Delft University of Technology (TUD, the Netherlands), and Ecole Polytechnique Fédérale Lausanne (EPFL, Switzerland) have formed a research cluster that exploits a synergy of field, laboratory and numerical methods in order to gain closer insight

into bio-physical interactions in meandering streams. The joint research program titled "Environmental Fluid Dynamics Laboratory in the Field" includes field studies on the rivers Spree, Tollense, Mulde (all three rivers in Germany), and Ledra (Italy). These rivers allow investigation to be carried out under a wide range of controlling variables as channel curvature, flow rates, riverbed and floodplain material (Blanckaert et al. 2009).

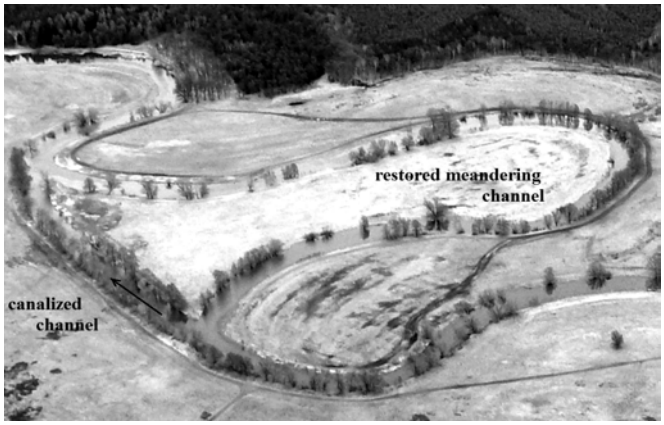

Figure 1. Aerial view of a river revitalization site on the Spree River near Möchwinkel in Germany.

In this paper we report preliminary results of a detailed field study of mean and turbulent flow structure completed in a meander bend of the lowland Spree River in Germany. The analysis is focused on: (1) the cross-sectional patterns of principal statistical characteristics of flow; (2) spatial variation of the patterns induced by the curvature of the channel; and (3) comparison of measured data with available analytical models.

2 FIELD MEASUREMENTS

2.1 *River reach*

Field measurements for this study were carried out in a reach of the Spree River near the village of Neubrück in Germany. The Spree River is a typical lowland river about four hundred kilometers in length, running from the Lusatian mountains through several shallow lakes to Berlin, where it joins the Havel River. Historical maps, as for instance "Lauf des Spree Strohms von Cossenblad über Beeskow und Fürstenwalde, und von Wusterhausen bis Berlin " dated 1796 from Berliner Hauptarchiv, indicate that during the pre-industrial period the channel of the Spree River was meandering practically on all its length (Nikolaevich et al. 2004).

Measurements were completed on a river bend which was evidenced as a naturally formed by the comparative analysis of the historical and recent cartographic materials and the results of field surveys (Nikolaevich et al. 2004, Figures 4 and 5). This river bend has an arc angle $\alpha = 150°$, path length $S_m = 760$ m, bend wavelength $\lambda = 485$ m, and sinuosity $S_m / \lambda = 1.57$ (Figure 2). Hydraulic and morphologic characteristics of the flow and channel of the river are presented in Table 1.

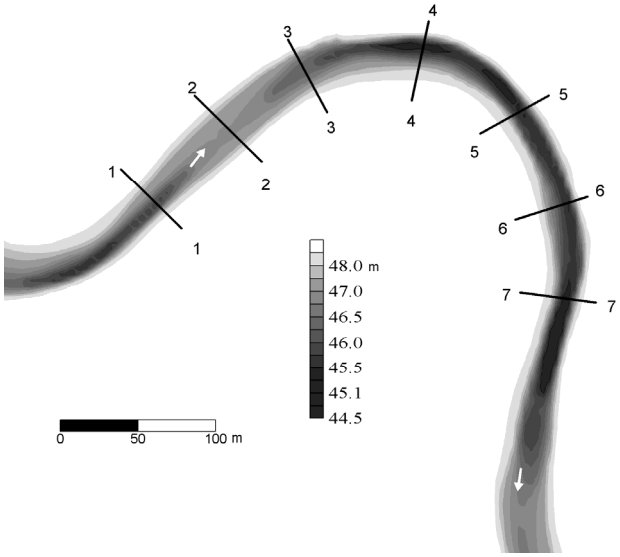

Figure 2. Bathymetry of the field site on the Spree River near Neubrück (arbitrary datum).

Table 1. Characteristics of field measurements

B, m	H, m	U, m	h_m, m	U_m, m/s	Re $\times 10^{-5}$	Fr
33.6	1.15	0.20	1.56	0.27	2.30	0.07
29.5	1.80	0.14	3.18	0.18	2.34	0.03

where B is river width, H is mean depth, U is bulk flow velocity, h_m is maximal depth in a cross-section, U_m is maximal velocity, Re is Reynolds number, and Fr is Froude number (first row is riffle and the second row is pool). The mean discharge during measurements was $Q = 7.5$ m^3/s and the slope of the free surface of the flow $S = 2.63 \times 10^{-5}$. The mean diameter of riverbed material is around 0.6 mm.

2.2 *Field equipment*

Measurements of 3-D mean and turbulent velocity fields were completed in this study with an acoustic Doppler velocimeter (ADV, Nortek AS). Individual ADV units were mounted using the equipment which was designed and manufactured in IGB (Figure 3). The basis of the mounting system is a portable platform made of aluminum profiles (1). Holders (2), secured to a plastic pad with clamping screws, enable traversing of the devices along the platform and positioning with a proper heading while tribrach screws (3) of the

holders provide an accurate vertical alignment of a guiding rod (4) and respectively of the ADV sensors (8). A 50 cm long beam (5) removes the sensor from the area of possible backwater effect. Another end of the beam houses the ADV signal conditioning module (9). The beam together with an ADV sensor and conditioning module can be moved along the guiding rod using a deploying rod (6) and fixed at a desired flow depth with a screw (7). Lateral vibration of the sensor can appear when a deployment depth is more than 2 m and the flow velocity is larger than 20 cm/s. Chains (10) attached to the sides of the beam and tightened to the platform were effectively used to prevent lateral vibration of the sensor.

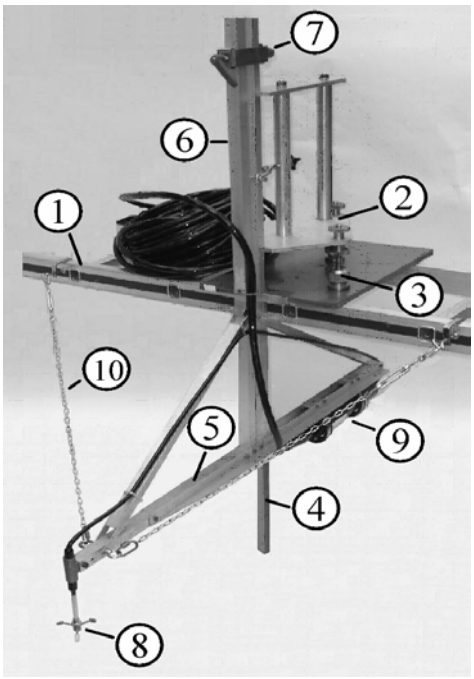

Figure 3. Field mounting equipment for ADV.

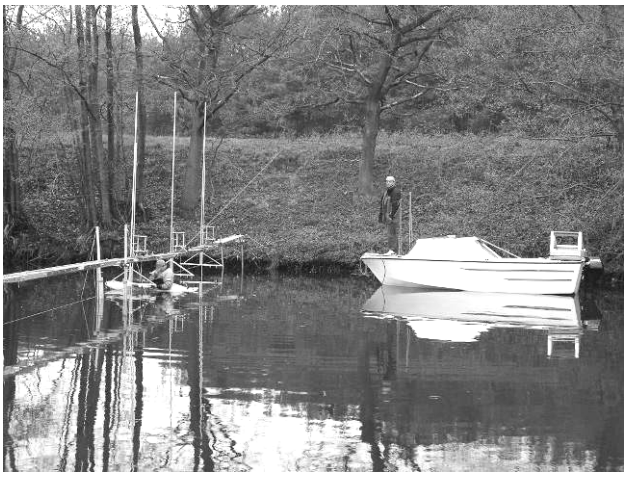

Figure 4. Measuring equipment and setup.

2.3 *Program of measurements*

The main purpose of the experimental program was to obtain detailed spatial patterns of mean and turbulent flow characteristics on a river reach. Seven cross-sections were designed and constructed along the river reach (Figure 2). The design of the cross-sections assumed uniform distribution of cross-sections along the reach and orientation of the cross-sections in a curvilinear system of coordinates. The construction of cross-sections was assisted by accurate positioning of benchmarks (1 m long steel pipes molded into a concrete pillow) with a laser total station.

Temporal bridges were built at every cross-section prior to the measurements (Figure 4). The bridges spanned a half width of the river at a time leaving the second half for navigation. After completion of the measurements in the first half part of the cross-section, the bridges were relocated to the second half. Correct alignment of each ADV holder in the curvilinear coordinate system was achieved by tuning the orientation of a plastic pad of ADV holders with the help of a total station.

Measurements were completed by an array of three ADV units operated synchronously (Figure 4). Three-dimensional velocity vectors were collected in 7 cross-sections uniformly distributed along the meander path. In each cross-section from 12 to 20 vertical profiles each composed of 11 measuring points were measured. The sampling period was 240 s for each point at the sampling rate of 25 Hz. Deployment of the devices was assisted from a support boat - a rodeo kayak; the ADV devices were interfaced to the portable computer on a base boat (Figure 4).

Water levels were monitored manually every hour during the measurements on the three gauging stations located at the upstream, middle, and downstream sections of the river reach. Local depth of the flow was measured with a sounding road. Samples of riverbed material were collected manually by a diver.

3 RESULTS AND ANALYSIS

3.1 *Theoretical background*

Centrifugal forces that develop in a curved channel produce superelevation of the water surface along the outer bank of the channel, which generates a counteracting pressure-gradient force. Local imbalances between these forces over the flow depth produce outward motion at the surface, downward motion along the outer bank and upward, lateral motion along the bed. The resulting pattern of helical motion redistributes

momentum shifting the zone of maximum streamwise velocity towards the concave bank near the bend apex. In a curvilinear system of coordinates with r (radial), θ (tangential), and z (vertical) coordinates, dynamical equations are presented in the following form (Rozovskii 1957):

$$u_r \frac{\partial u_r}{\partial r} + \frac{u_\theta}{R}\frac{\partial u_r}{\partial \theta} + w\frac{\partial u_r}{\partial z} - \frac{u_\theta^2}{R} = -gS_r + \frac{\partial}{\partial z}\left(\nu_t \frac{\partial u_r}{\partial z}\right) \quad (1)$$

$$u_r \frac{\partial u_\theta}{\partial r} + \frac{u_\theta}{R}\frac{\partial u_\theta}{\partial \theta} + w\frac{\partial u_\theta}{\partial z} + \frac{u_r u_\theta}{R} = gS_\theta + \frac{\partial}{\partial z}\left(\nu_t \frac{\partial u_\theta}{\partial z}\right) \quad (2)$$

where u_r, u_θ, and w are radial, tangential, and vertical mean velocities, R is radius of curvature, and S_r, S_θ are radial and tangential slopes. The system (1) – (2) can be solved analytically for the radial component, which represents the secondary currents, if the distributions of tangential velocities and of turbulent viscosity are presented in an analytical form. For natural streams with large radii of channel curvature the distribution of mean velocities usually differs little from the logarithmic law and the parabolic distribution $\nu_t = \kappa u_* z\sqrt{1 - z/h}$ for ν_t applies, then

$$u_r = \frac{1}{\kappa^2} U_\theta \frac{h}{R}\left[F_1(\eta) - \frac{\sqrt{g}}{\kappa C}F_2(\eta)\right], \quad (3)$$

$$F_1(\eta) = \int_0^1 \frac{2\ln\eta}{\eta - 1}d\eta, \text{ and } F_2(\eta) = \int_0^1 \frac{\ln^2\eta}{\eta - 1}d\eta$$

where C is Chezy coefficient, g is specific gravity, h is flow depth, u_* is shear velocity, U_θ is depth-averaged tangential velocity, κ is von Karman parameter, and $\eta = z/h$.

3.2 *Mean flow structure*

Measured depth-averaged mean velocity vectors (u_θ, u_r) show a pattern which is characteristic for flow in bends with self-formed alluvial channels (Figure 5). Initially asymmetrical and skewed toward the outer bank of the upstream bend, flow in cross-section 1 gradually transforms into relatively symmetrical and accelerated stream over the riffle in the cross-section 2. As the flow inters the meander bend it became skewed again toward the outer bank (cross-section 3). Magnitude of velocity became significantly reduced over the pool area where flow attains strongly asymmetrical shape (cross-section 4). Further downstream velocities also appear reduced near both the outer and inner banks of the bend (cross-section 5) indicating the flow separation zones. Similar patterns remain in the downstream part of the bend (cross-sections 6 and 7) where the secondary pool is located (Figure 2).

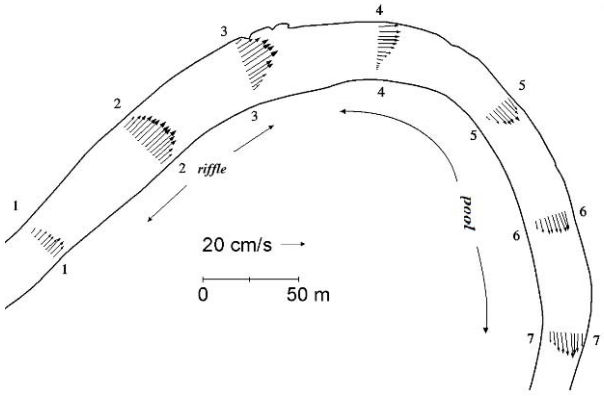

Figure 5. Depth-averaged mean velocity vectors.

Typical distributions of tangential velocity components in the cross-sections are illustrated in Figure 6. It can be seen that the structure of the mean flow over the riffle (cross-section 2) resembles pattern similar to the open-channel flow (Sukhodolov et al. 1998). Maximal velocities are located near the free surface and in the central part of the channel. Velocities are gradually decreasing toward the riverbed and banks. Patterns of flow in the pool area of the bend exhibit progressive shift in the location of velocity maxima towards the outer bank and at the same time towards the mid depth of the flow (cross-sections 4 and 6). The phenomenon of deepening of velocity maxima is a well- known and characteristic feature of flow in In the pool area the vectors display classical pattern of secondary spiraling flow with a large gyre occupying almost whole cross-section and rotating towards the outer bank (cross-sections 4 and 6). Near the outer bank flow displays a smaller counter-rotating gyre similar to those observed in laboratory flows (Mockmore 1943, Kondart'ev et al. 1959, Thorne and Hey 1979, Blanckaert and Graf 2004). Comparison of the patterns for primary (tangential) and secondary (radial and vertical) flows indicate that maxima of the primary flow are located at the outer margins of large-scale secondary gyres while the centers of the gyres are located at the mid-channel.

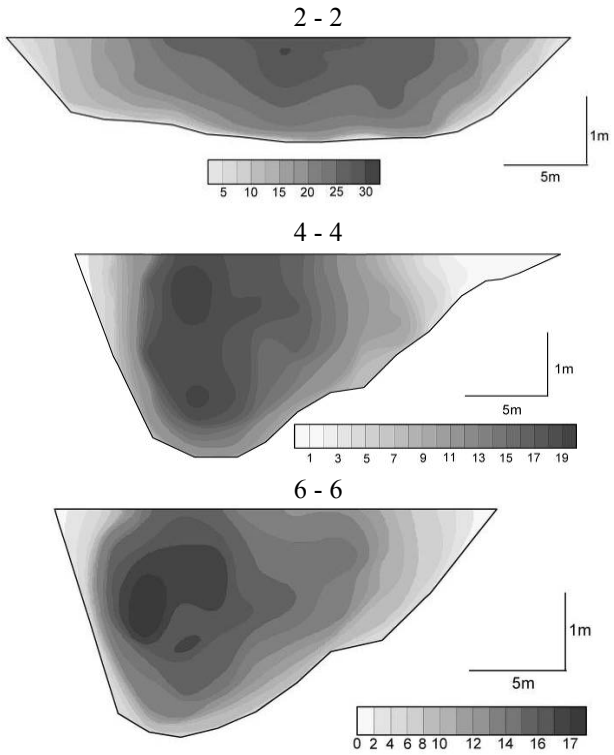

Figure 6. Time-mean tangential components of velocity vector (velocity scale is in cm/s).

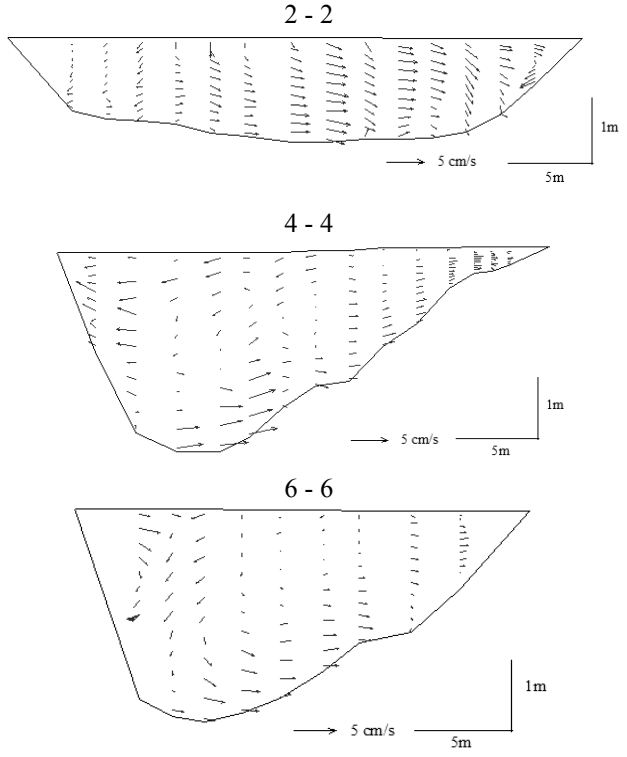

Figure 7. Time-mean $V(u_r, w)$ velocity vectors.

3.3 Turbulent flow structure

Analytical solution (3) for vertical distribution of radial velocity is obtained using parabolic distribution of turbulent viscosity $v_t = -\overline{u'_\theta w'}/(\partial u_\theta / \partial z)$ and logarithmic distribution of tangential velocity (Rozovskii 1957). This also implies that Reynolds stresses $-\overline{u'_\theta w'}$ are distributed linearly in the vertical plane similarly like in the open channel flow

$$-\frac{\overline{u'_\theta w'}}{u_*^2} = 1 - \frac{z}{h} \qquad (4)$$

Patterns of $-\overline{u'_\theta w'}$ measured at the riffle (cross-section 2) of the meander bend (Figure 8) show that the shear stresses are distributed in good correspondence with the linear model (4). Their maxima are located near the riverbed and gradually decrease to zero values near the free surface. In the cross-sections located at the pool area, the patterns of $-\overline{u'_\theta w'}$ indicate that zero values are attained beneath the free surface of the flow (cross-section 4) and that values of the shear stress became negative at some areas coincident with the locations of the upper parts of the secondary flow cells (cross-section 6, Figure 8).

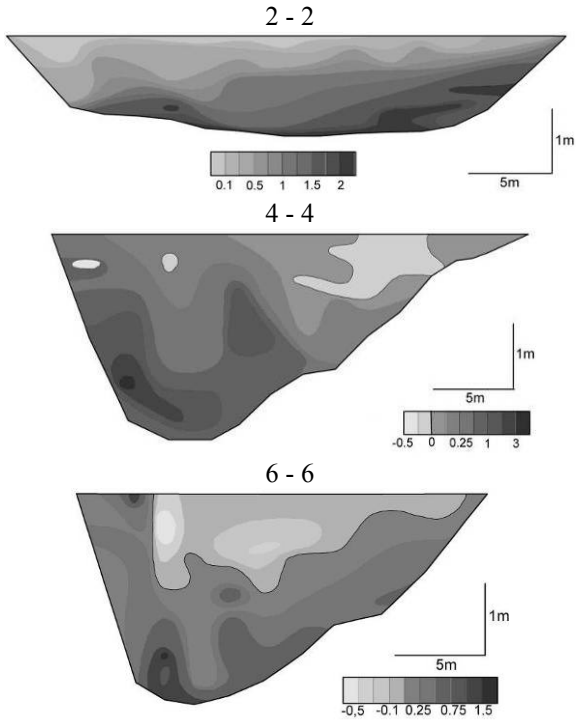

Figure 8. Patterns of $-\overline{u'_\theta w'}$ (kinematic units cm^2/s^2).

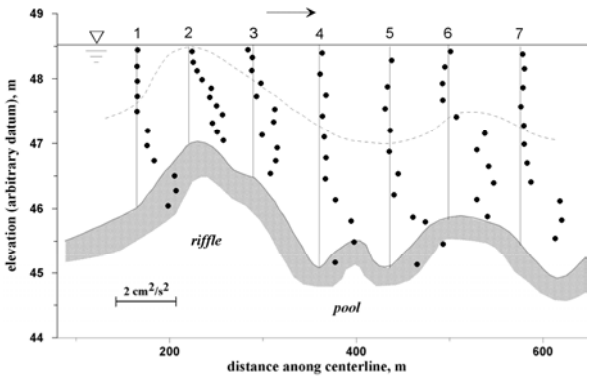

Figure 9. Pattern of $-\overline{u'_\theta w'}$ along the river centerline.

Figure 9 shows vertical profiles of $-\overline{u'_\theta w'}$ measured on the verticals in the centerline of the

river. The dashed line in Figure 9 marks the positions of zero values of $-u'_\theta w'$. Vertical profiles measured over the riffle area display a segmented pattern that is attributed to the effect of small-scale morphological features – sand waves on the riverbed (Sukhodolov et al. 2006, Blettler et al. 2010). Although vertical distribution of $-u'_\theta w'$ measured in the pool area deviate systematically from linear relation (4), their shape reveal a qualitative agreement with the shape of distributions measured in recent studies in schematized laboratory setups (Blanckaert 2009).

Patterns of shear stresses in the riffle area, except near left bank, are indicative of relative uniformity of shear stress distribution in the lateral direction. Near the left bank the flow is affected by the separation at the apex of the upstream meander bend. In the pool area the maximal shear stresses are observed at the foot of the outer bank and slightly over the deepest place of the pool. The stresses greatly reduce over the inner bank slope of the point bar and in the areas very near the bank they are practically zero (Figure 8).

Horizontal components of turbulent stresses $-u'_\theta u'_r$ are formed either by friction on the banks or at the inte *Meanders, secondary flow, hydrodynamics, turbulence, shear layers* rfaces of flows of different velocities as for example between the main flow in the river and recirculating flow in separation zones.

Horizontal components of the shear stresses $-u'_\theta u'_r$ measured in representative cross-sections of the river are shown in Figure 10. In symmetrical channels turbulent stresses $-u'_\theta u'_r$ are maximal near the river banks and are zero at the center plane which represents the plane of symmetry (Sukhodolov and Sukhodolova 2010). Such pattern is characteristic for the flow over the riffle zone of the bend (cross-section 2). In this section $-u'_\theta u'_r$ is nearly zero in the central part of the channel while near the banks two areas of $-u'_\theta u'_r$ which are comparable in the magnitude to $-u'_\theta w'$ are present (Figure 10).

In the pool the pattern of $-u'_\theta u'_r$ is no more symmetric and skewed towards the outer bank. Although at the apex of the bend (cross-section 4) the zero values of the stresses are located near the centerline of the stream, the zone of zero stresses is stretching over the slope of the point bar (Figure 10). Furthermore, in the apex the zone of maximal $-u'_\theta u'_r$ is located at the area of maximal depth and hence is collocated with the lower part of the cell of secondary circulation. The largest values of lateral stresses are measured at the outer bank at the presurface area and it is collocated with the outer bank cell of secondary flow (Mockmore 1943, Rozovskii 1957, Blanckaert and de Vriend 2005). Further downstream (cross-section 6) the plane of symmetry with zero $-u'_\theta u'_r$ shifts towards the inner bank and a zone of slight non-zero stresses appears attached to the inner bank (Figure 10). The symmetry plane is shifted because of flow separation in the bend downstream the apex. The separation was clearly depicted by a zone of reverse flow in the cross-section 5 and in the cross-section 6 by a vertical shear layer with enlarged values of $-u'_\theta u'_r$ (Figure 10).

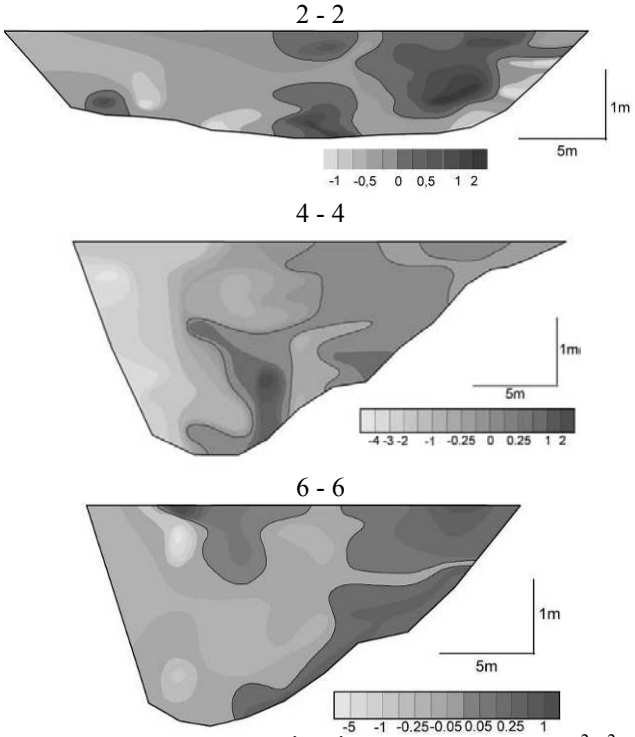

Figure 10. Patterns of $-u'_\theta u'_r$ (kinematic units cm^2/s^2).

Integral insight into the spatial arrangement of turbulence structure and locality of energy sources is provided by the distributions of turbulent kinetic energy (Figure 11). It can be seen that in the riffle area (cross-section 2) the maximal values of $k = 0.5\left(u'^2_\theta + u'^2_r + w'^2\right)$ were measured near the riverbed and they are much smaller near the free surface of the flow. The transition from large to smaller values is gradual (cross-section 2). In the pool area there are two sources of turbulent energy. The most prominent and primarily related to the friction over the riverbed is depicted by a band of increased values near the foot of the outer bank (cross-sections 4, and 6). Near the bend apex the secondary source of energy is collocated with the counter-rotated smaller gyre (cross-section 4). In the *Meanders, secondary flow, hydrodynamics, turbulence, shear layers* downstream sections of the pool the secondary source of energy is produced by the lateral shear layer at the flow separation zone (cross-section 6). The magnitude

of this source is even exceeding the magnitude of the bed-friction (Figure 11).

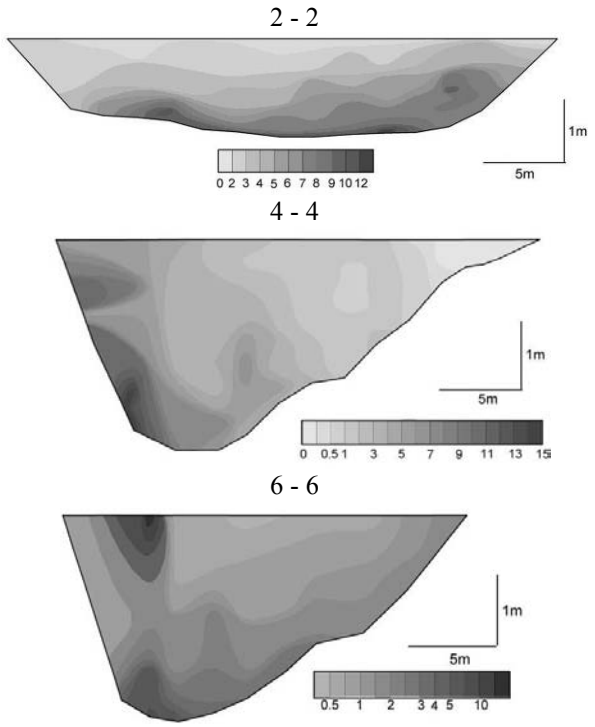

Figure 11. Turbulent kinetic energy k (in cm^2/s^2).

4 DISCUSSION AND CONCLUSIONS

The results of the study show that the structure of mean and turbulent flow in the meander bend is essentially three dimensional and highly heterogeneous. This complexity of flow naturally raises the concern on the applicability of the analytical approach (3) of Rozovskii (1957) which is based on the assumption that shear stress is linearly distributed over the depth (4), tangential velocity follows the logarithmic law while the eddy viscosity is parabolic.

This study shows that in the pool sections, where the influence of flow curvature is significant, the shear stresses are greatly redistributed in the vertical plane and also laterally. The shear stresses cannot be correctly predicted by the equation of uniform flow (4) and their accurate assessment also requires to account for radial component of shear stress tensor $-u'_r w'$ in agreement with the recent laboratory studies by Blanckaert (2009). However, the shear velocities can be estimated from local vertical profiles of $-u'_\theta w'$ by linearly extrapolating the linear relationship (4) into the near bed region. This approach was used in this study.

The patterns of mean velocity (Figure 6) are also suggestive that the logarithmic law cannot hold over the entire vertical profile and only can be valid near the riverbed in agreement with previous studies of Booij (2003). Moreover, the shift of velocity maxima into flow core and near bed region is the precondition for the development of adverse velocity gradients that will affect the vertical distribution of turbulent viscosity (Booij 2003).

We used the obtained values of shear velocities, mean tangential velocity computed from the vertical velocity profiles and the value of $\kappa = 0.41$ to make predictions of vertical distributions of tangential velocities according to (3). The results of computations for some representative vertical profiles measured in the central parts of cross-sections 4, 5, and 6 are presented in Figure 12. It can be seen that predictions of Rozovskii (1957) method is in relatively good agreement with the measured data. Mostly strongest deviations between predicted and measured values can be concluded for the lower parts of the velocity profiles. These deviations are most probably due to strong influence of the riverbed roughness. Thus, despite of some violations in basic assumptions underlying Rozovskii (1957) method it is capable of reasonable accurate predictions. However, the question what makes the method so robust – the insensitivity of the model to the parameters perturbation is still not clear and requires further study. Some clue to this question is provided already in the monograph by Rozovskii (1975) who in the absence of accurate measurements of shear stresses applied methods of indirect estimates from the velocity profiles and used values of κ in the range from 0.38 to 0.94 (Rozovskii 1957, p. 143, Figure 67). Obtained data sets offer unique opportunities for testing of different approaches and techniques with the benefits of independent estimates of turbulent and mean flow characteristics. Our further work on the analysis of the data and interpretation will also include methods of numerical modeling for testing the assumptions and implications of the study for ecological research.

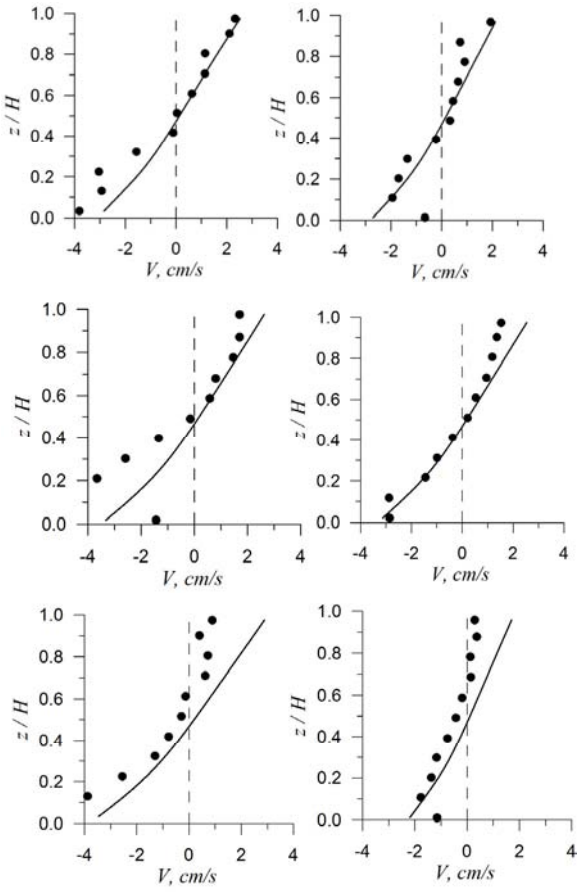

Figure 12. Comparison of measured and predicted secondary currents.

ACKNOWLEDGEMENTS

Nicholas Nikolaevich and Sergey Maltsev are thanked for the assistance with field measurements. The financial support of the study was provided through the grants SU 405/3 and DN66-149 from the Deutsche Forschungsgemeinschaft and the Netherlands Organization for Scientific Research.

REFERENCES

Blanckaert, K. (2009), "Saturation of curvature-induced secondary flow, energy losses, and turbulence in sharp open-channel bends: Laboratory experiments, analysis, and modeling." J. Geoph. Res., Vol. 114, F03015, doi:10.1029/2008JF001137.

Blanckaert, K., Schnauder, I., Sukhodolov, A. van Balen, W., and Uijttewaal, W.S.J., (2009), "Meandering: field experiments, laboratory experiments, and numerical modeling." In: River, Coastal and estuarine Morphodynamics. C. Vionnet, M.H. Garcia, E.M. Latrubesse, and G.M.E. Perillo (eds.), Proc. of the 6th Symposium, September 2009, Santa-Fe, Argentina, 863-875.

Blanckaert, K. and de Vriend, H.J. (2005), "Turbulence structure in sharp open-channel bends." J. Fluid Mech., Vol. 536, 27-48.

Blanckaert, K. and Graf, W.H. (2004), "Momentum transport in sharp open-channel bends." J. Hydraul. Eng., Vol. 130(3), 186-198.

Blettler, M., Sukhodolov, A.N. and Tockner, K. (2010), "Hydraulic conditions over bed forms control the benthic fauna distribution in a lowland river (Spree River, Germany)." In: Proc. of RiverFlow 2010. (submitted).

Booij, R. (2003), "Modeling the flow in curved tidal channels and rivers." In: Int. Conf. On Estuaries and Coasts, November 9-11, Hangzhou, China, 786-794.

Fargue, L. (1868), "Etude sur la correlation entre la configuration du lit et la profondeur d'eau dans les riveres a fond mobile." Annales des Ponts et Chaussees, Vol. 38, 34-92.

Kondrat'ev N.E., Lyapin, A.N., Popov, I.V., Pin'kovskii, S.I., Fedorov, N.N. and Yakunin, I.I. (1959), Channel Processes, Hydrometeoizdat, Leningrad.

Mockmore, C.A. (1943), "Flow around bends in stable channels. " Trans. ASCE, Vol. 109, 593-628.

Nezu, I. and Nakagawa, H. (1993), Turbulence in Open-Channel Flows, Balkema, Rotterdam, The Netherlands.

Nikolaevich, N., Sukhodolov, A. and Engelhardt, C. (2004), "Assaying historical maps and relict channel forms for the analysis of channel processes (on example of the Spree River in Germany)." In: RiverFlow 2004, , M. Greco, A. Carravetta & Della Morte (eds.), A. Balkema, Vol. 1, 181-189.

Rozovskii, I.L. (1957), Flow of water in bends of open-channels. Academy of Sciences of Ukraine, Kiev.

Seminara, G. (2006), "Meanders." J. Fluid Mech., Vol. 554, 271-297.

Sukhodolov, A. and Sukhodolova, T. (2010) "Case Study: Effect of submerged aquatic plants on turbulence structure in a lowland river." J. Hydraul. Eng., (in press).

Sukhodolov, A., Fedele J. and Rhoads B. (2006), "Structure of flow over alluvial bedforms: an experiment on linking field and laboratory methods." Earth Surface Proc. and Land., Vol. 31, 1292-1310.

Sukhodolov, A., Thiele, M. and Bungartz H., (1998), "Turbulence structure in a river reach with sand bed." Water Resources Research, Vol. 34, 1317-1334.

Thorne, C.R. and Hey, R.D. (1979), "Direct measurements of secondary currents at river inflexion point. " Nature, Vol. 280, 226-228.